AN APPARATUS FOR MEASURING THE LOW FREQUENCY DYNAMIC CHARACTERISTICS OF MATERIALS.

Francis OLIVIER* and Mona KHOURY

Centre d'Etudes et de Recherches pour la Discrétion Acoustique des Navires (CERDAN)
DCN Toulon, 83800 Toulon Naval, FRANCE

INTRODUCTION

The TNO Institute of Applied Physics at Delft (TPD Netherland) has developed an apparatus for the evaluation of dynamic stiffnesses of resilient mounts and flexible hosepipes (see reference) used in automotive or shipboard machinery. It exploits accelerometric transfer measurements and, as main advantages, allows to work under static preload with a hydraulic jack, and over six possible degrees of freedom. We have adapted it to the characterization of the intrinsic properties of materials in a low frequency range (from 100 Hz up to about 2 kHz) through the longitudinal bulk $M = \lambda+2\mu$ and the shear $G = \mu$ complex moduli.

In that paper we describe this apparatus, its main characteristics and performances. We also present some results and explain its limitations in order to propose some improvements. They show how the TPD bench may be considered as an interesting and complementary device for the knowledge of foam and composite rubbery materials, at low frequencies, under varying conditions of static pressure.

* External consulting engineer from STERIA for CERDAN; telephone : (33) 94-02-50-53

I - GENERAL WORKING PRINCIPLES

I - 1 General description

The TPD apparatus is a steel made heavy framework composed of a lower bench supporting an arch which carries a hydraulic jack (figure 1-a). It has sufficiently large dimensions to receive metal masses of several hundreds kilograms, that one can isolate from the structure by hanging them on resilient mounts. Usual work needs to superpose two masses related together by the element to be tested like a resilient mount or a flexible hose. Generally these masses have a cicular shape; they are chosen within a set of several steel or aluminium masses which inertial characteristics and internal eigenfrequencies are perfectly known. So one can build a discrete mass-stiffness-mass system (figure 1-b), isolated by suspensions judiciously chosen between a set of known mounts, and obviously much less stiff than the element to test. By changing masses and isolators stiffnesses, we are able to control the working frequency broadband while satisfying the "isolated discrete system" assumption. In special cases, this broadband may go from a few tens of hertz up to about 2 kHz.

For vibratory testing of elastic mounts or flexible hosepipes, it is often interesting to put them in real working situation. This is the reason why the TPD bench includes a jack and a hydraulic circuit, both hand operated with their own pump. With the first, one can apply a static loading that simulates a real structure or a machine which may weigh up to a hundred tons. The second allows filling a flexible pipe with a liquid pressure.

The mass-stiffness-mass system is aligned along the vertical z-axis. The horizontal plane will be noted xy. The excitations are applied with two electrodynamic shakers, symmetrically mounted on a transversal bar (y) which is perpendicular to the main frontbeam (x). They attack the upper mass, named input mass and pointed out by index 1. The vibration goes through the element to test, down to the lower output mass pointed out by the index 2.

I - 1 Vibratory equations for the 6 degrees of freedom system

One can consider that the mount to test behaves like a pure stiffness if one admits the following realistic assumptions :

- its mass is negligible compared to the masses 1 and 2;
- its dimensions are much smaller than the wavelength (especially for low frequencies);
- it presents a linear behavior for vibrations having little displacements.

Writing Hooke's law between the two bounds of the specimen and generalizing it to the six possible degrees of freedom, one can define its stiffness 12x12 matrix [K] as :

$$\{F\} = [K] \cdot \{X\} \quad \Leftrightarrow \quad \begin{Bmatrix} \{F_1\} \\ \{F_2\} \end{Bmatrix} = \begin{bmatrix} [K_{11}] & [K_{12}] \\ [K_{21}] & [K_{22}] \end{bmatrix} \cdot \begin{Bmatrix} \{X_1\} \\ \{X_2\} \end{Bmatrix} \qquad (1)$$

- $\{F_i\}$ force vector on node i, with 6 components : 3 forces F_x, F_y, F_z, and 3 torques M_x, M_y, M_z;
- $\{X_i\}$ displacement vector on node i, with 6 components : 3 translations x, y, z, and 3 rotations θ_x, θ_y, θ_z;
- $[K_{11}]$ et $[K_{22}]$ input (respectively output) stiffness matrix for blocked output (respectively blocked input);
- $[K_{12}]$ et $[K_{21}]$ input (respectively output) transfer matrix for blocked output (respectively blocked input).

This matrix contains all the mount characteristic stiffnesses. From now on it will be the unknown of our general problem. We will consider all of its elements as complex values which imaginary parts reveal the eventual presence of damping.

Using that formulation, one can write the dynamic equation of the two-nodes discrete system :

$$[M]\{\ddot{X}\} + [K]\{X\} = \{F_e\} \tag{2}$$

where $\{F_e\}$ is the six components external force vector applied to the input mass with the two shakers, and [M] is the inertial tensor on both nodes. If we consider the two masses as punctual, that is if the two junction nodes merge into the centers of gravity of the masses, then [M] is a diagonal matrix which twelve diagonal elements may be written as : m_1, m_1, m_1, J_{x1}, J_{y1}, J_{z1}, m_2, m_2, m_2, J_{x2}, J_{y2}, J_{z2}. For example, J_{yi} is the moment of inertia of node i (i =1 or 2) around the y rotation axis.

In practice, we do not use the whole formulation in every cases. Except for inertias, all the involved variables may depend on frequency so that it would be too long to process them all systematically. To lighten the problem formulation, one can take advantage of the symmetry properties of matrix [K] due to the reciprocity theorem. Therefore we are allowed to concentrate only on the output mass movements and to consider that $[K_{21}]$ and $[K_{22}]$ contain the whole characteristic stiffness informations about the specimen. Moreover, since we apply excitations to the input node (mass n°1), the equation of the output node becomes simpler setting its second member to zero :

$$[M_2]\{\ddot{X}_2\} + [K_{21}]\{X_1\} + [K_{22}]\{X_2\} = \{0\} \tag{3}$$

To go on into simplifications, another working fundamental assumption is to suppose the output blocked. In practice, we realize that condition by using an output mass much heavier that the input one (for example m_1 = 50 kg and m_2 = 450 kg). In the following paragraph, we will verify the validity of such an approximation which intends to eliminate a third term in equation (3) and reduce it to:

$$[M_2]\{\ddot{X}_2\} + [K_{21}]\{X_1\} = \{0\} \tag{4}$$

From this equation we can notice that the unknown is restricted to $[K_{21}]$ and deduce two important remarks that will affect the experimental aspect of our method. First, since external forces have disappeared we will not have to measure them. The measurements will be reduced to displacements or accelerations, and this leads to the second remark. The "blocked output" hypothesis may seem quite paradoxal because, strictly, we should measure zero output accelerations! In fact the assumption remains true if one satisfies the following compromise : output accelerations must be measurable, that means stronger than the background noise, but much weaker than the input ones (about 20 dB).

The transfer matrix $[K_{21}]$ is generally not fullfilled. It may present many zero elements, depending on the specimen shape. This represents a considerable advantage for our method, because we may reduce the number of unknowns from it. In other words, symmetries may occur in the mount shape, which tend to separate coupled degrees of freedom. Therefore the formulation becomes simpler and, for example, in case of a specimen having three planes of symmetry xy, xz and yz, equation (4) becomes :

$$\begin{Bmatrix} m_2\ddot{X}_2 \\ m_2\ddot{Y}_2 \\ m_2\ddot{Z}_2 \\ J_{x2}\ddot{\theta}_{x2} \\ J_{y2}\ddot{\theta}_{y2} \\ J_{z2}\ddot{\theta}_{z2} \end{Bmatrix} = \begin{bmatrix} K(1,1) & 0 & 0 & 0 & K(1,5) & 0 \\ 0 & K(2,2) & 0 & K(2,4) & 0 & 0 \\ 0 & 0 & K(3,3) & 0 & 0 & 0 \\ 0 & K(2,4) & 0 & K(4,4) & 0 & 0 \\ K(1,5) & 0 & 0 & 0 & K(5,5) & 0 \\ 0 & 0 & 0 & 0 & 0 & K(6,6) \end{bmatrix} \cdot \begin{Bmatrix} X_1 \\ Y_1 \\ Z_1 \\ \theta_{x1} \\ \theta_{y1} \\ \theta_{z1} \end{Bmatrix} \qquad (5)$$

I - 3 Tension-compression equations along z axis.

By construction, the experimental mounting privileges vertical (z) tension-compression vibrations within all other degrees of freedom. Equation (5) shows that this "dof" is not coupled with any other one, so that it becomes very easy to write this two-nodes reduced system equations for harmonic vibrations :

$$\begin{aligned} m_1\ddot{Z}_1 + K(Z_1 - Z_2) &= F_e \exp(i\omega t) \\ -K(Z_1 - Z_2) + m_2\ddot{Z}_2 &= 0 \end{aligned} \qquad (6)$$

where $K = K(3,3)$. The two angular eigen frequencies are given by :

$$\omega^2 = 0 \quad \text{et} \quad \omega^2 = K\left(\frac{1}{m_1} + \frac{1}{m_2}\right) \qquad (7)$$

and since $\ddot{Z} = -\omega^2 Z$, both displacements are written as :

$$Z_1 = F_e \frac{K - m_2\omega^2}{\omega^2 (m_1m_2\omega^2 - K(m_1+m_2))} \quad \text{et} \quad Z_2 = F_e \frac{K}{\omega^2 (m_1m_2\omega^2 - K(m_1+m_2))} \qquad (8)$$

The output/input ratio leads to :

$$\frac{Z_2}{Z_1} = \frac{K}{K - m_2\omega^2} = \frac{1}{1 - \frac{m_2}{K}\omega^2} = \frac{\ddot{Z}_2}{\ddot{Z}_1} \qquad (9)$$

From transfer function (9) we can observe that, for a given specimen stiffness, the heavier the output mass the weaker its acceleration is, compared to the input mass one. This contrast increases with frequency and for small stiffnesses. This illustrates the previous paragraph purpose and shows how the question of signal to noise ratio may appear. For that reason, we will probably have to deal with high frequency limitations. Moreover we can notice that the stiffness K may be approximated by :

$$K = - m_2 \omega^2 \frac{\ddot{Z}_2}{\ddot{Z}_1} \qquad (10)$$

with a negligible error when $m_2\omega^2/K >> 1$. Therefore, simply multiplying the accelerometric transfer function by $-m_2\omega^2$, provides directly a good estimation of the stiffness. To evaluate the specimen damping, we just have to take the complex K phase information into account.

We just saw that signal to noise ratio problem could cause the high frequency limits of our approach. Other reasons may be :
- unsatisfaction of the "discrete system" assumption at the eigenfrequencies neighbourhood;
- bad isolation of the tension-compression degree of freedom which may get coupled with other ones like rotation, in case of small defects or weak dissymmetries in the mounting.

According to (9), the low frequency limit will be given by :

$$f = \frac{1}{2\pi}\sqrt{\frac{K}{m_2}} \qquad (11)$$

These considerations we just made about tension-compression may be applied to the other degrees of freedom in the same way. But neither the involved stiffnesses and inertial terms, nor the frequency limitations therefore, would be the same.

I - 4 Experimental processing.

Measuring the accelerometric transfer function between the two masses in the conditions described above, needs a good experimental care.

To guarantee that the degrees of freedom are sufficiently uncoupled from each other, all the transducers, shakers as well as sensors, are used by pairs, geometrically symmetric or antisymmetric mounted depending on the dof (figure 1-b). That kind of rig allows spurious movement cancellation and desired movement extraction. Each pair needs twin transducers, very well calibrated in modulus and phase, so that their signal

may be added or substacted without distorsion. These operations are made by two analog electronic devices (see the right part of figure 1-b) :
- the VCCD (Vibration Component Cancellation Device) splits the input amplificated signal into two in-phase or phase opposit components which feed the two electrodynamic shakers (Denitron);
- the ASD (Additive Substractive Device) gives on output the half-sum or half-difference (following the operator choice) of both input signals coming from a pair of sensors.
For vertical tension-compression (z axis), both vibrators are fed by the same signal, and the ASD compute the half-sum of the amplified signal outcoming from the pairs of accelerometers.

About signal processing, we usually estimate transfer function (9) with a HP 6532 numeric analyser, which can also provide the excitation signal. To optimize the Fourier analysis in the point of view of signal to noise ratio, we use a slowly swept sine which may require about seven minutes acquisition time when working from 0 to 2 kHz with a 2.5 Hz resolution. This quite long analysis allows the output signal to come into view from the background noise level, while avoiding at the same time, the injection of a too powerful excitation which could introduce undesirable non linear behaviour. Then we satisfy the following compromise : noise level $< Z_2 << Z_1$.

The digitalized transfer function migrates out from the analyzer into the memory of a HP 9000 computer which makes post-processings like, for example, the multiplication by $-m_2\omega^2$ and the graphics too. A complete software program manages the whole tests over many kinds of specimen like mounts, hoses and pipes. It can also process a matrix treatment to separate coupled degrees of freedom.

To insure that the experimental conditions fullfill the working assumptions described in the paragraph above, we generally add complementary measurements to the main transfer function. They are (figure 2) :
- the measurement of both input and output masses acceleration spectra, to verify that the level of the second is effectively about 20 dB lower than the level of the first; we can also see if they are eventually polluated by a spurious movement.
- the measurement of this spurious degree of freedom to diagnostic and correct it;
- the measurement of the bench acceleration spectrum, below the output mass; it must be at least 10 dB lower than the output mass level for the discrete system to be well isolated. Because of a bad resilient suspension, it could happen that the output mass might be excitated not only by the specimen but through the isolation mount too. Indeed an acoustical channel links it to the input mass : it goes up through the upper mount to the jack, then from the jack down to the lower part of the bench and up again through the lower mounts to the mass. This case may occur if, for example under very heavy static loadings, the resilient mounts lose their efficiency because of smashing or their own degradation.

Moreover, we can use many different amplification gains on the excitation signal, to verify that the specimen has effectively a linear vibratory behavior in Hooke's law.

II - USING TPD BENCH AS A VISCOANALYZER

II - 1 Measurement of longitudinal and transverse moduli

We have explained how to measure the dynamic stiffnesses of a resilient specimen. Now we are going to decribe a derivated usage of TPD bench, specifically destinated to the evaluation of the M longitudinal bulk (plane wave) and G transverse (shear) moduli which are characteristic of the material the specimen is made of. Elasticity theory says that those two parameters are sufficient to completely define an isotropic material. This may be extended to viscoelastic materials by considering their moduli as complex values. From now on, we will not speak of a mount to test anymore, but of a material specimen, and our objectives will not be anymore to evaluate only global parameters like stiffnesses, but to obtain a material intrinsic information, which does not depend on the mount shape.

This special utilization of the apparatus is particularly well adapted to the characterization of materials like natural or synthetic rubbers, foams and many of their derivated composites which may contain inclusions or internal structures. As main advantage it provides directly the viscoelastic moduli we use to deal with in acoustical modeling, either with Lamé coefficients in tridimensional elasticity equations, or through the sound celerities of longitudinal and transversal waves :

$$M = \lambda + 2\mu \; ; \; G = \mu \;\Rightarrow\; c_L = \sqrt{\frac{\lambda+2\mu}{\rho}} \;\text{ et }\; c_T = \sqrt{\frac{\mu}{\rho}} \qquad (12)$$

In that point of view, the direct method we recommend here is much more appropriate than the usual viscoelastic measurement devices like rheovibrons or viscoanalysers, which generally try to estimate Young's and shear moduli, E and G, through the observation of beams working in tension-compression, torsion or flexion. In using the equations linking the elastic moduli to each other, a simple analytical calculation of the relative error is sufficient to convince oneself about it . If we deduce M from experimental values of E and G, we obtain :

$$M = G\left(\frac{4G-E}{3G-E}\right) \;\Rightarrow\; \frac{dM}{M} = \frac{dG}{G} - \frac{E\,G}{(3G-E)(4G-E)}\left[\frac{dG}{G} - \frac{dE}{E}\right] \;\Rightarrow$$

$$\frac{\Delta M}{M} = \left(1 + \frac{E\,G}{(3G-E)(4G-E)}\right)\frac{\Delta G}{G} + \frac{E\,G}{(3G-E)(4G-E)}\frac{\Delta E}{E} \qquad (13)$$

By another way using Young's modulus and Poisson ratio ν we have :

$$M = E\frac{(1-\nu)}{(1+\nu)(1-2\nu)} \;\Rightarrow\; \frac{\Delta M}{M} = \frac{\Delta E}{E} + \frac{2\nu^2(2-\nu)}{(1-\nu^2)(1-2\nu)}\frac{\Delta\nu}{\nu} \qquad (14)$$

The materials we are used to study, generally have quite strong Poisson coefficients between 0.4 and 0.5. A well-known consequence of that fact is the following inequality :

$$G = \frac{E}{2(1+\nu)} \quad \Rightarrow \quad 2.8\,G \leq E \leq 3\,G \tag{15}$$

In expressions (13) and (14) of $\Delta M/M$, the presence of (1-2ν) or (3G-E) in the denominators shows how a small error in evaluating E and/or ν may be amplified on M :

$$\begin{aligned} &- \nu = 0.4 \;\Rightarrow\; \frac{\Delta M}{M} = 5\frac{\Delta G}{G} + 4\frac{\Delta E}{E} = \frac{\Delta E}{E} + 3\frac{\Delta \nu}{\nu} \\ &- \nu = 0.45 \;\Rightarrow\; \frac{\Delta M}{M} = 10\frac{\Delta G}{G} + 9\frac{\Delta E}{E} = \frac{\Delta E}{E} + 8\frac{\Delta \nu}{\nu} \end{aligned} \tag{16}$$

Figure 3 illustrates the consequence of that fact on the longitudinal wave celerity. An error of 1% in the measurement of E or G may produce an error of 10% or 20 % on M. 1% is a quite optimistic error because many viscoelastic devices have very poor accuracy which sometimes lead to aberrations like E > 3 G!

II - 2 Specific tool for measuring M = λ+2μ.

For measuring a material longitudinal bulk modulus, we most often use square panel shaped samples, from 30 to 50 mm thick, with 100 mm, 200 mm or 300 mm sides. Other tests also work with cylinders of same thickness and nominal diameters of 80 mm or 140 mm. These dimensions are needed with an accuracy of ± 3 mm, so that the specimen can fit a metal box which encloses it and blocks its lateral displacements. By pressing weakly on its sides and lubricating the lateral contact faces with a silicon oil, we are sure to block both static and dynamic displacements along x and y axis; this also allows free tangential sliding parallel to z axis. The blocking box is made of a steel circular plate which supports a square framework with two fixed faces and two moving ones which may be actionned with a screw. This tool weight is about 50 kg and is not negligible so that it must be added to the output mass. To apply the excitation correctly, a metal piston of lightly smaller section compared to the specimen, is put between its upper face and the input mass (figure 4).

This care we take in the mounting, insures the dynamic condition which is said of "plane deformation". Along the vertical z axis, the stress-strain relation for the specimen considered as an element of volume, may be written as :

$$\sigma_{zz} = \mu\,(\varepsilon_{xx} + \varepsilon_{yy}) + (\lambda + 2\mu)\,\varepsilon_{zz} \tag{17}$$

Since the tool cancels the lateral displacements one can merge :
- the z stress into the output inertial force divided by the sample section S;
- the z strain into the gradient of z displacements divided by the sample thickness h.

Then, using (10) and (17) one can write :

$$\lambda + 2\mu = \frac{\sigma_{zz}}{\varepsilon_{zz}} = \frac{m_2 \ddot{Z}_2 / S}{(Z_2 - Z_1)/h} = K(3,3)\ \frac{h}{S} \qquad (18)$$

Therefore we can see that the measurement of the longitudinal bulk modulus only requires to correct the stiffness K(3,3) with the shape factor h/S which is very easy to evaluate because the specimen shape cannot change. In addition to the good control of boundary conditions, this is a second advantage of the method. For data processing the estimation of M requires to apply this second coefficient to the accelerometric transfer function besides the factor $-m_2\omega^2$ already used for the estimation of the stiffness. The obtained value (figure 5) may be complex in case of damping, and may depend on frequency if the material exhibits a dispersive behavior.

II - 3 Static preloading configuration.

The TPD bench allows the testing of materials under static preloading which may be useful for certain applications. Under pressure the materials behave differently : their internal static stress state makes them look like other materials with a weakly higher density (a few percent) but much stronger elastic moduli. The relationship between pressure and those moduli is generally not linear and depends a lot on the kind of considered material. For homogeneous materials the molecular interactions are changed. For composites or foams the internal structures are affected.

To simulate the working under static pressure we use the hydraulic jack. A force ring gives the value of the injected force up to 100 tons, and therefore, dividing it by section S, the value of the static pressure. Because of the blocking framework, S does not change. The thickness h may eventually diminish under the effect of smashing : anyway its new value can be easily measured by comparison with its initial state. As it was said before, the specimen shape remains the same and the shape factor is calculated as before.

Some aspects may change on the experimental point of view. Since the specimen stiffness increases (figure 1-b), so does the low frequency limit and the accelerometric contrast fades between input and output masses on one hand, and between the output mass and the lower part of the bench on the other hand. So the isolation mounts are generally removed into more resisting ones which support heavy preloading and are consequently less efficient. Coupling with other dof may also become more embarrassing and polluate the measurements. Only the signal to noise ratio takes advantage of that configuration. Nevertheless one can observe that the experimental conditions get globally worse (figures 2-c and 2-d) but the measurement remains always possible for static pressures less than 20 bars.

About static preloading configuration, an important remark must be done. The static stress we apply is not isotropic but axial. Therefore, the stress state inside the

specimen is not isotropic either. Indeed, for a material with a static Poisson ratio ν, its components are :

$$\sigma_{xx} = \sigma_{yy} = \sigma_{zz} \frac{\nu}{1 - \nu} \tag{19}$$

For instance the blocking frame reaction is 66% of preloading if $\nu = 0.4$ and 82% if $\nu = 0.45$. So there is some ambiguity in interpreting the results obtained in such a configuration, mixing static and dynamic considerations.

If the dynamic modulus variation is due to the isostatic stress state, we probably underestimate the real value of M that the material would present under isotropic preloading (in a fluid for instance). Nevertheless equation (19) shows that the materials with a strong Poisson ratio like rubbers, are not very affected. About materials with weak Poisson ratio like rubbery foams, one can imagine that their compressibility makes the Poisson ratio increase under the effect of heavy preloading. The Poisson ratio of a foam is rather low at atmospheric pressure because of the bubbles it contains. A static smashing may fill those cavities where the material will not expand anymore : so it becomes less compressible. To conclude, we can say that the error must probably decrease as the static pressure increases, and be more sensitive for the lighter loadings which unfortunately, are the conditions we are most often used to deal with.

II - 4 Shear measurement

Measuring the shear modulus G can be done in a way similar to that used for the longitudinal bulk modulus. It only needs to work along the horizontal x axis instead of the vertical z axis (figure 6-a). We then look after evaluating K(1,1) which may be obtained by transposing the relations concerning K(3,3) (cf. §I-3). The application of the shape factor remains the same because the equation linking the dynamic stiffness to the characteristic modulus is of the same kind as (18) :

$$G = \mu = \frac{\sigma_{zx}}{\varepsilon_{zx}} = \frac{m_2 \ddot{X}_2 / S}{(X_2 - X_1)/h} = K(1,1) \frac{h}{S} \tag{20}$$

If the measurement principle does not make any difficulty, on the other hand the experimental conditions are much less easy. The shear mounting presents some specificities very different from those of vertical tension-compression, which involve difficulties on several aspects.

First, the pairs of transducers must be horizontally positioned, diametrally and phase opposite. Since the shear modulus of a material is always much weaker than the longitudinal one, the global shear stiffness of a specimen is much lower too. Therefore the acceleration transmitted through the specimen to the output mass has a lower level, and the signal risks to be drowned very soon at a few hundred Hz, into the background noise. In such a case we will have to use a lighter output mass (figure 6-b).

Another problem is that the panel cannot be held in the blocking frame because the definition of shear requires to keep its edges free. As a consequence we lose some control on the boundary conditions and the shape factor when we want to work under heavy static preloading. If not enclosed in a box, the sample can expand on its sides : then its thickness strongly decreases, its section increases and its lateral faces round off, so that the shape factor becomes uneasy to evaluate. A second consequence is the difficulty to well isolate the shear degree of freedom, even without static preload. Indeed, the lack of signal mentioned above may lead to amplify the excitation signal. Then the x displacements tend unfortunately to get coupled with the rotation around y axis, especially for the highest frequencies (figure 6-b). To improve this particuliar point two solutions are possible.

The first one is to mount a special rig that would be mechanically and geometrically symmetric toward the medium plane which horizontally cuts the input upper mass through the middle (figure 6-a). But we then need a second twin specimen and a second mass identical to the lower one which movements would balance and cancel the rotation degree of freedom. But for practical reasons of heaviness and overcrowding this solution cannot be applied.

The second one keeps the original rig and concerns the measurement post-processing. Since a spurious rotation may occur we can take it into account by excitating it deliberately and measuring it. Then a matrix treatment may allow the separation of the different stiffness terms involved in the problem. Let us consider the output mass movements with both coupled degrees of freedom ; if m is its mass and J its moment of inertia around the y axis shifted to the junction point with the sample, then following (5) one can write :

$$\begin{aligned} m\,\ddot{X}_2 &= K(1,1)\,X_1 + K(1,5)\,\theta_{y1} \\ J\,\ddot{\theta}_{y2} &= K(5,1)\,X_1 + K(5,5)\,\theta_{y1} \end{aligned} \qquad (21)$$

We do not have to measure an accelerometric transfer function anymore, but directly all the accelerations involved in (21), using for instance an electrical reference. These measurements must be done a first time by excitating the shear translation of the input mass (figure 6-a), and a second time by excitating its rotation applying a torque around y axis (figure 7-b). To do this we just have to put both electrodynamic shakers in the same vertical position used for tension-compression, but in that case they are fed with two phase-opposite signals (antisymmetric mounting). Then we are able to build a linear system of 4 equations and 4 unknowns which are the stiffness terms. A software program makes the matrix processing which has to provide theses complex values versus frequency. It often happens that the sample has a horizontal (xy) plane of symmetry : in such cases the calculation should yield this property of the stiffness matrix with K(1,5) = K(5,1). For practical reasons this method has not been tested yet for the shear modulus evaluation, but we know from elsewhere that it already works for resilient mounts testing at low frequencies.

CONCLUSION

We have described in that paper a derivated utilization of TPD bench in order to characterize the elastic properties of materials like rubbers and foams at low frequencies. This apparatus gives reliable results especially on the longitudinal bulk modulus under different conditions of static pressure. The shear measurements are not completely satisfying yet but there are some solutions to improve them.

Another interesting direction of investigation is to test the behavior of the measurements for various materials, especially viscoelastic ones which may exhibit strong damping (phase sensibility) and frequency dispersion (magnitude sensibility) in their transition region. Naturally the big dimensions of the TPD bench prohibit testings versus temperature like many viscoanalysers focused on the temperature-frequency equivalence law. But, even at room temperature, the possibility of working under different static pressures, with many kind of rubbers and composites, makes this special apparatus an efficient way of knowing those materials, complementary of other devices like viscoanalyzers and acoustic impedance tubes.

Reference

"Handbook on the measurement of sound transfer functions of flexible".
J.G. van Bakel ; Department of Ship Acoustics, TNO Institute of Applied Physics, Delft, Netherlands.

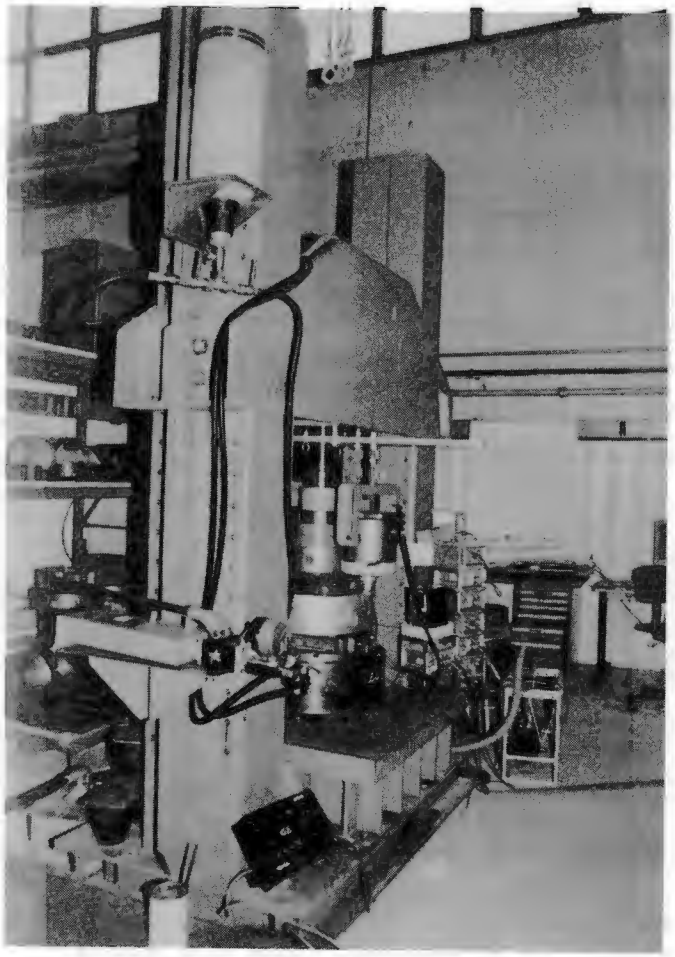

Figure 1-a : general view of TPD bench.

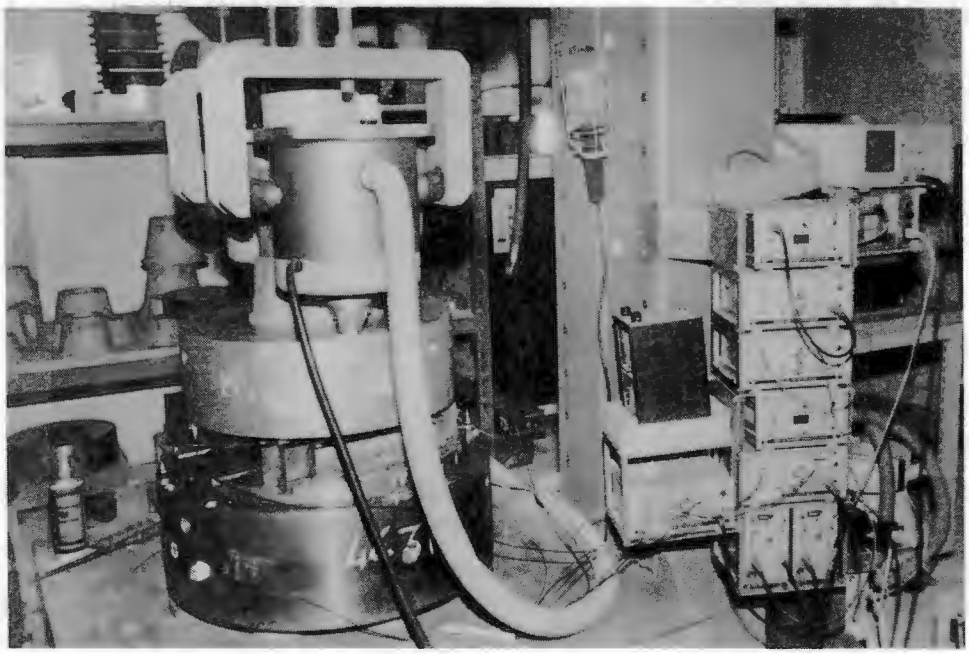

Figure 1-b : measurement rig with diametrally opposite transducers (see lower mass) connected to analog additives and substractive devices (ASD and VCCD on the right part of the picture).

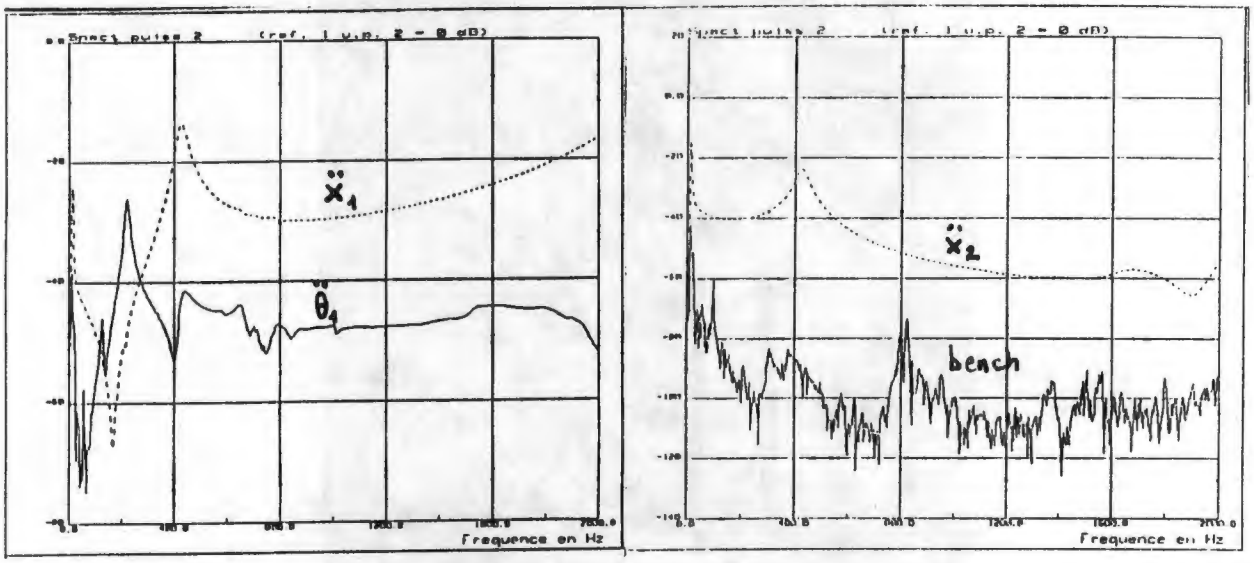

(a)

(b)

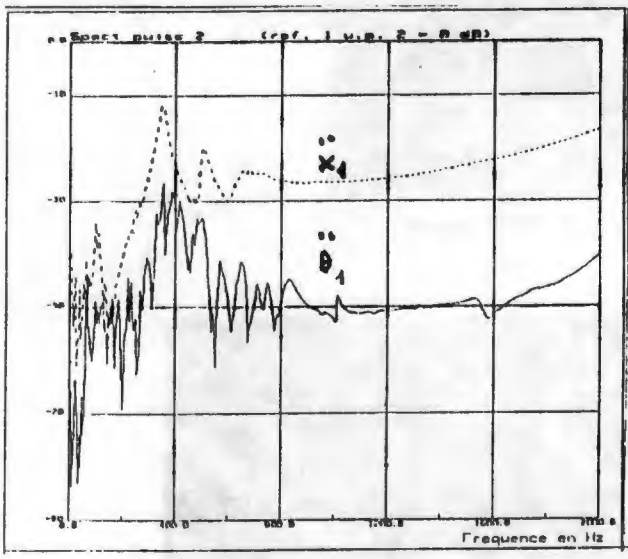

(c)

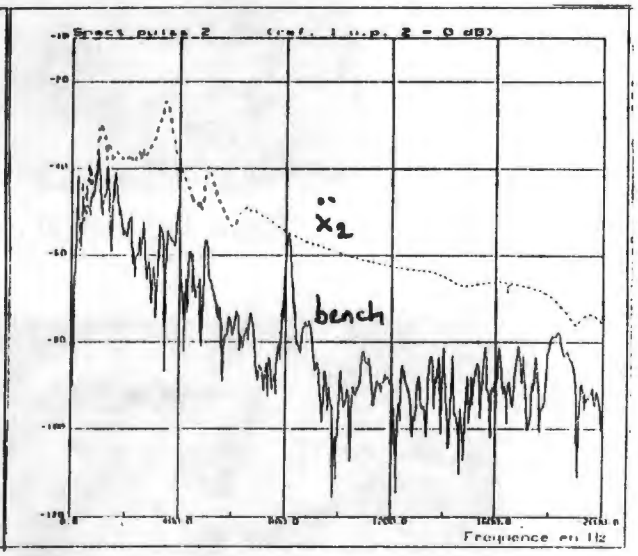

(d)

Figure 2 : control measurements for vertical tension-compression.

(a) input mass acceleration and spurious rotation; (b) output mass and lower part of the bench accelerations (the contrast checks the good isolation of the mounting).

(a) and (b) curves come from a testing under a static preloading of 1 bar; (c) and (d) are obtained for a preloading of 11 bars : one can notice the degradation on the experimental conditions.

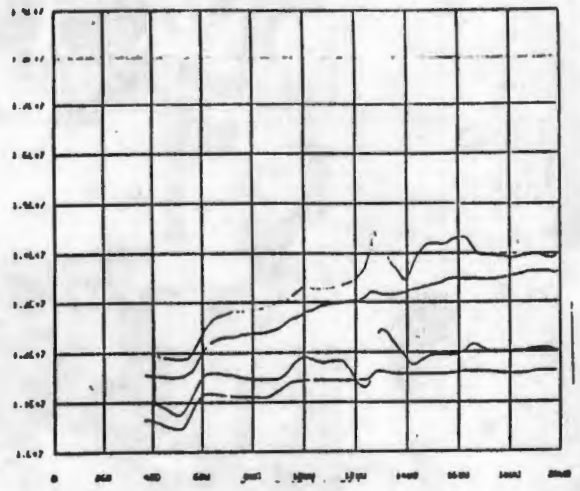

Frequency (Hz)

(a) : real part of Young's modulus (N/m^2)

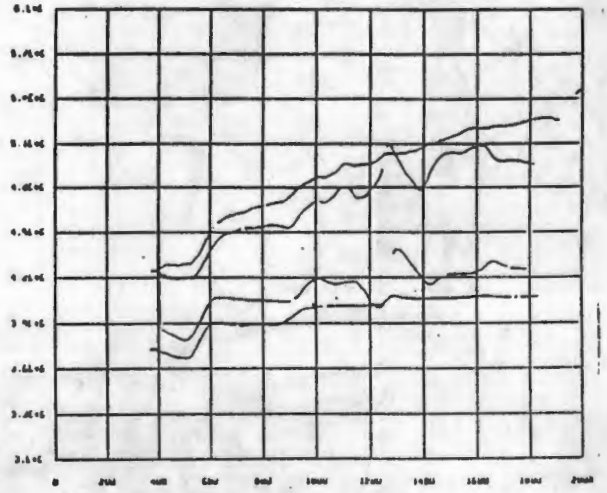

Frequency (Hz)

(b) : real part of the shear modulus (N/m^2)

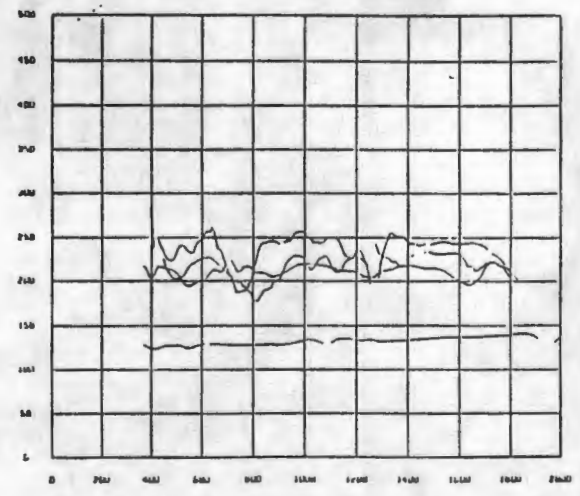

Frequency (Hz)

(c) : real part of the longitudial wave celerity $(\lambda+2\mu/\rho)^{1/2}$ (m/s)

Figure 3 : visco-analyser results for 4 cases of temperature and pressure. The specimen is a small beam in tension-compression for Young's modulus measurement (a), in torsion for the shear modulus (b). Using relations between elastic constants one deduce the longitudinal wave celerity (c).

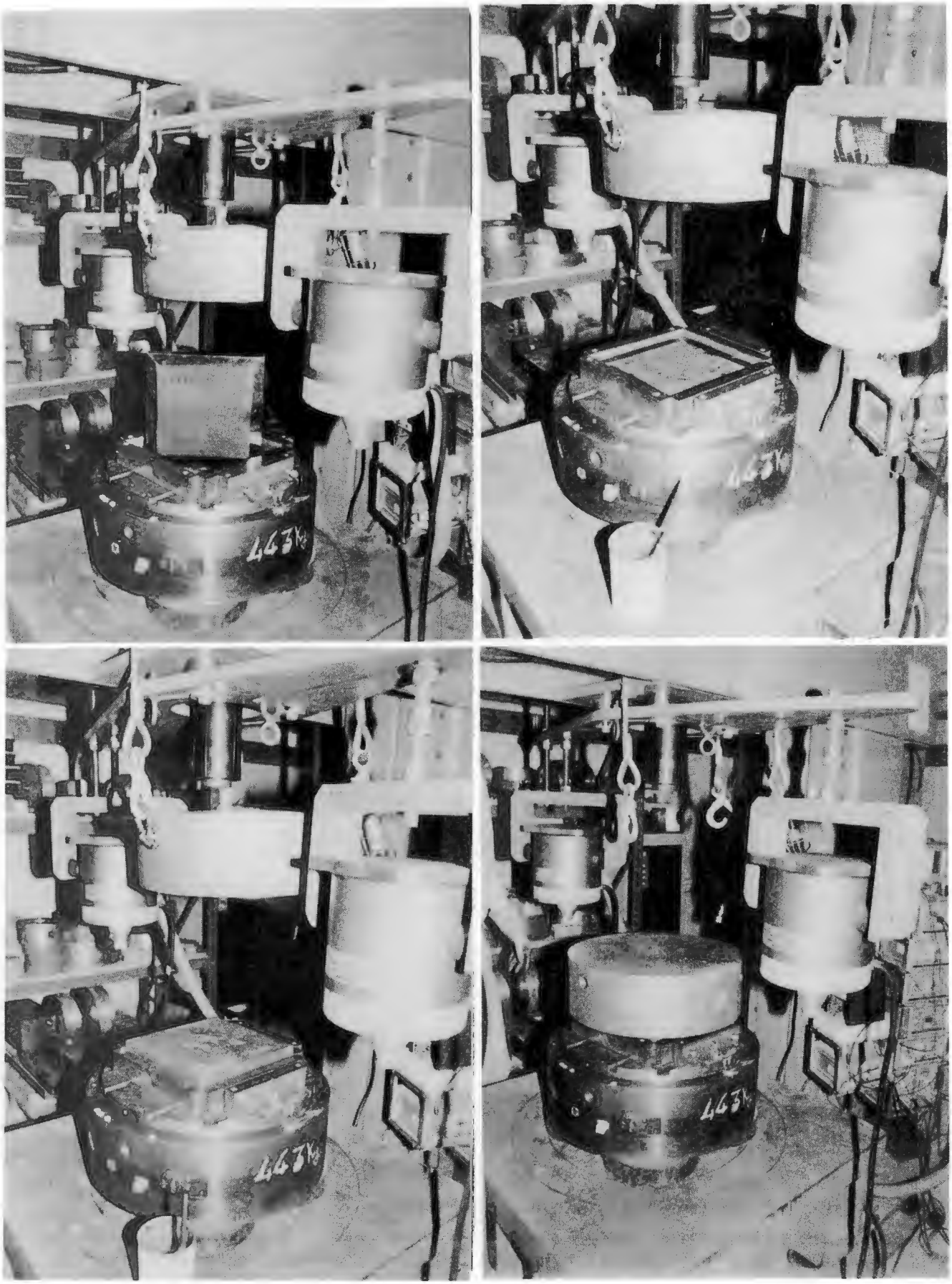

Figure 4 : installation of the square panel specimen. The square blocking framework (a) encloses the specimen (b). Then we superpose the plane excitation piston (c) and the input upper mass (d).

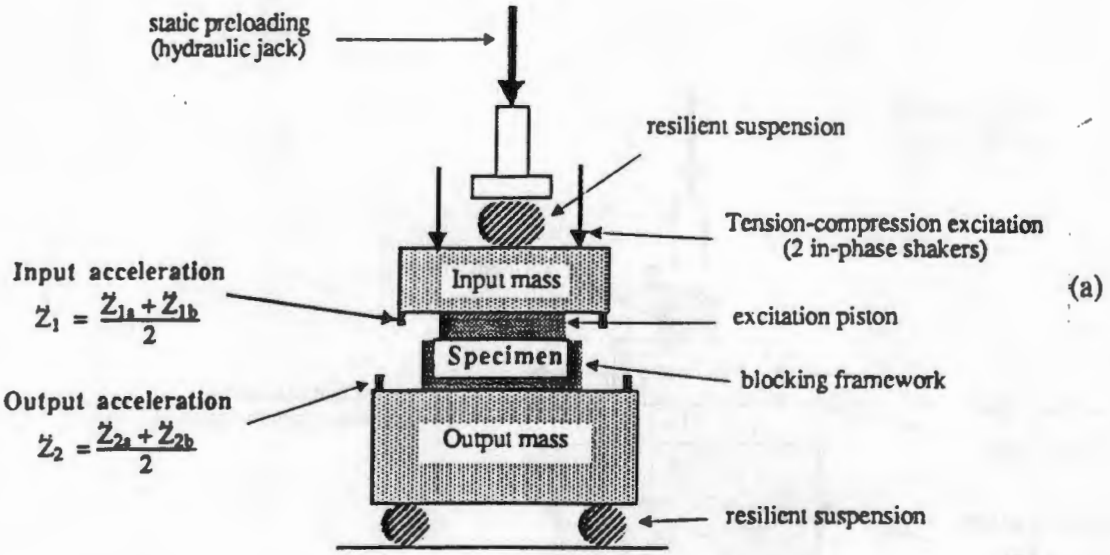

(a)

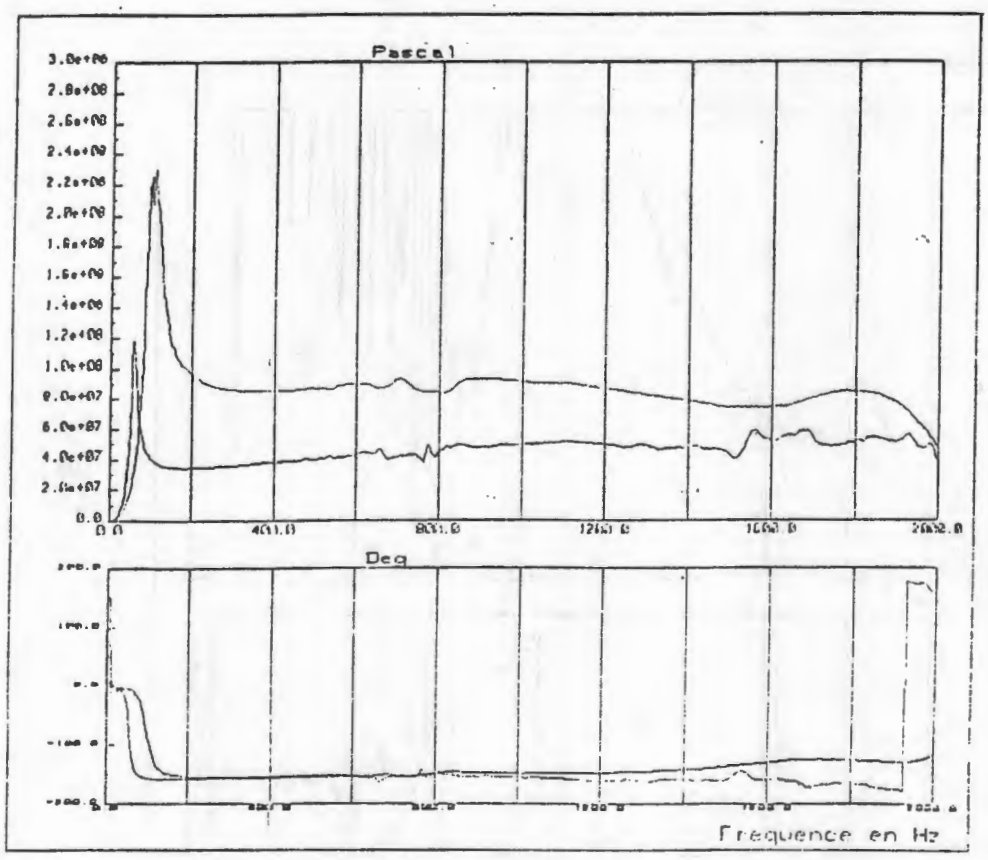

(b)

Figure 5 : measurement of the longitudinal bulk modulus $\lambda+2\mu$ (N/m^2). (a) : experimental mounting. (b) : resulting curves for a material under 1 bar and 8 bars static pressures. One can notice the significant flat part of the curves, the limitating low frequency resonance peak, and the 180° constant phase due to a sign error (true value 0°). Presence of damping would smooth the peak and shift the phase.

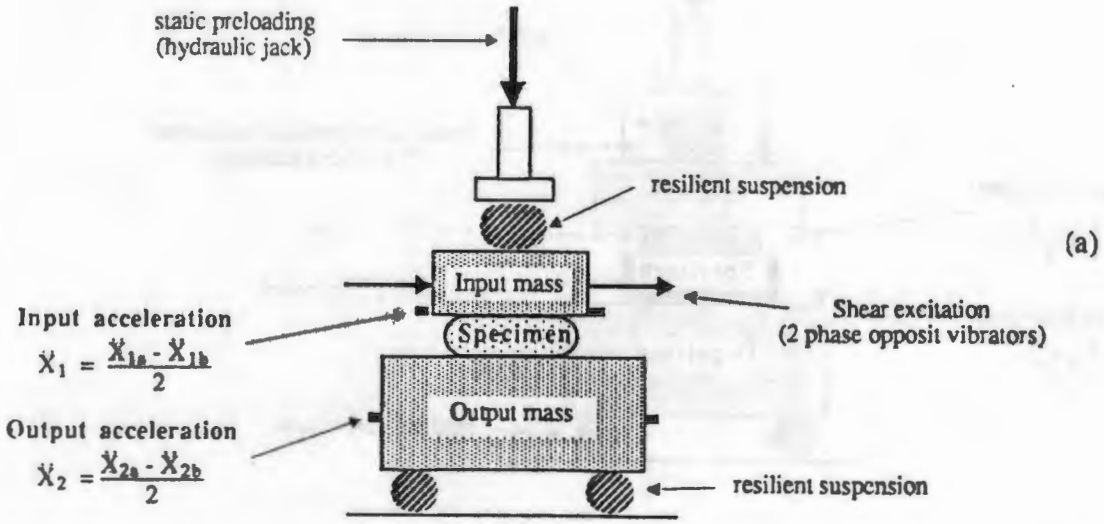

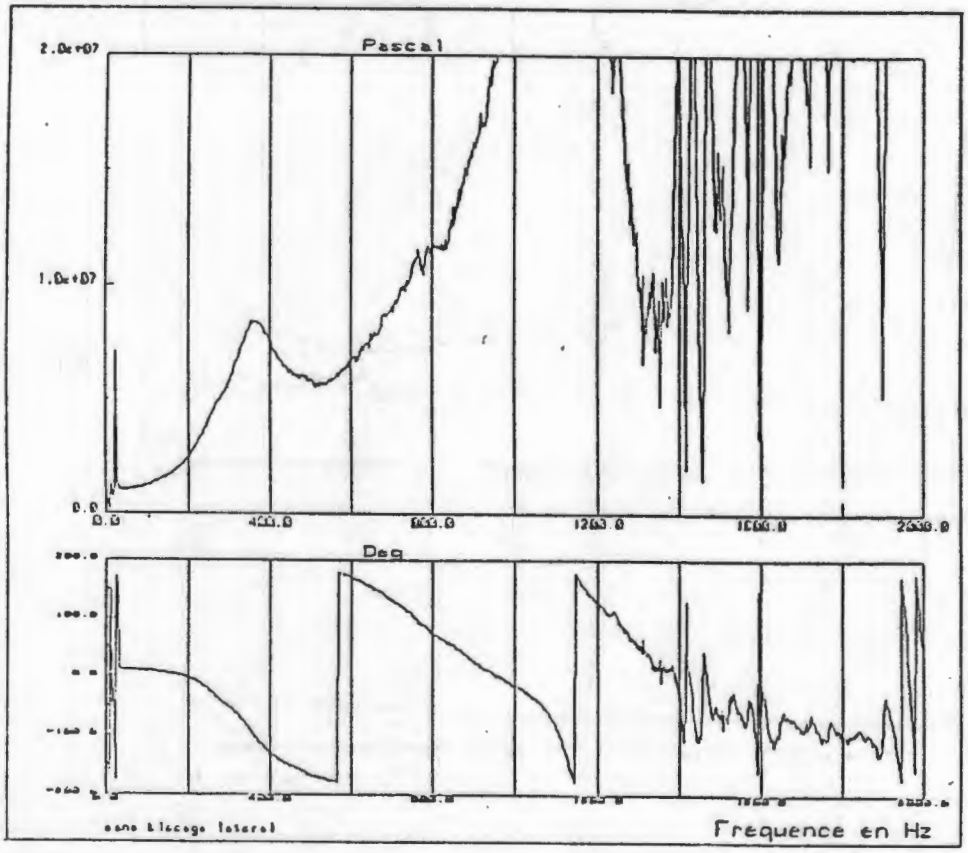

(b)

Figure 6 : measurement of the shear modulus (N/m^2). (a) : experimental mounting. (b) : resulting curve for a material at atmospheric pressure. One can notice the very low resonance peak due two a too heavy output mass. Background noise and spurious rotation peaks polluate this measurement from a hundred Hz.

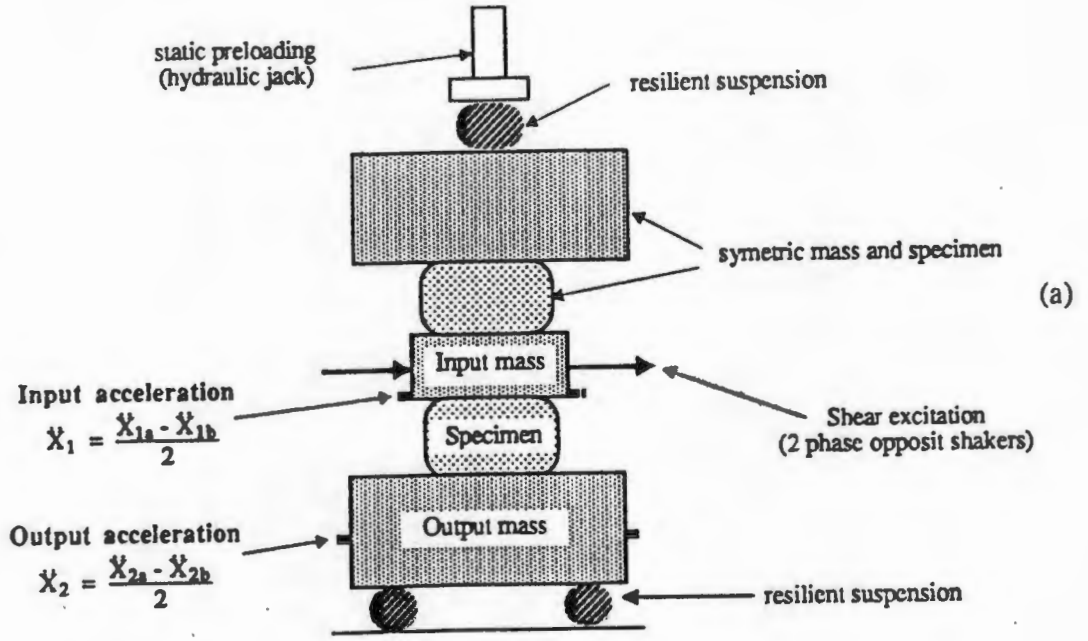

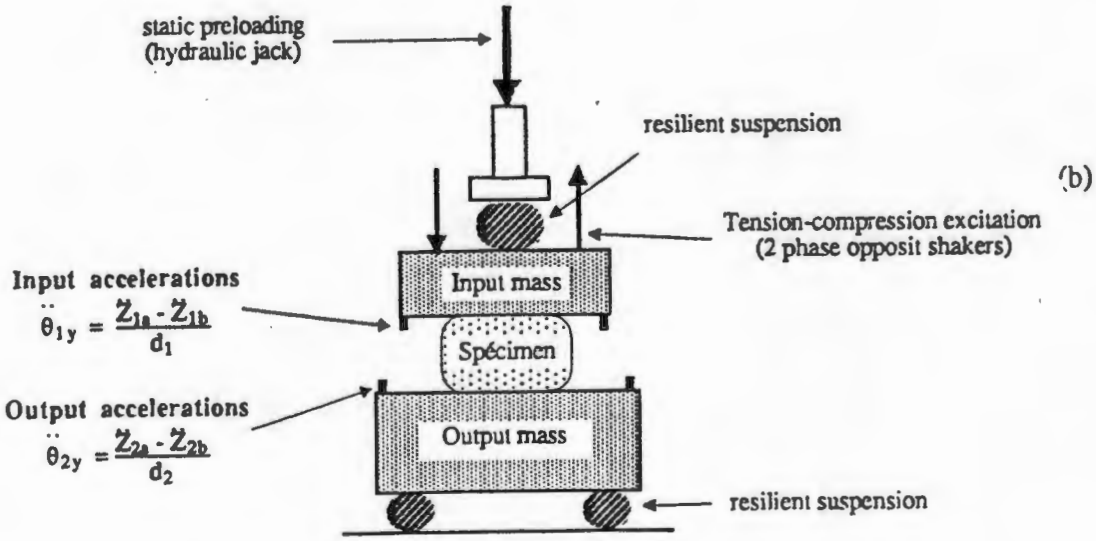

Figure 7 : (a) symmetric mounting for the shear modulus measurement. (b) mounting for the rotation stiffness measurement : it is the same as tension-compression but with phase opposite transducers.